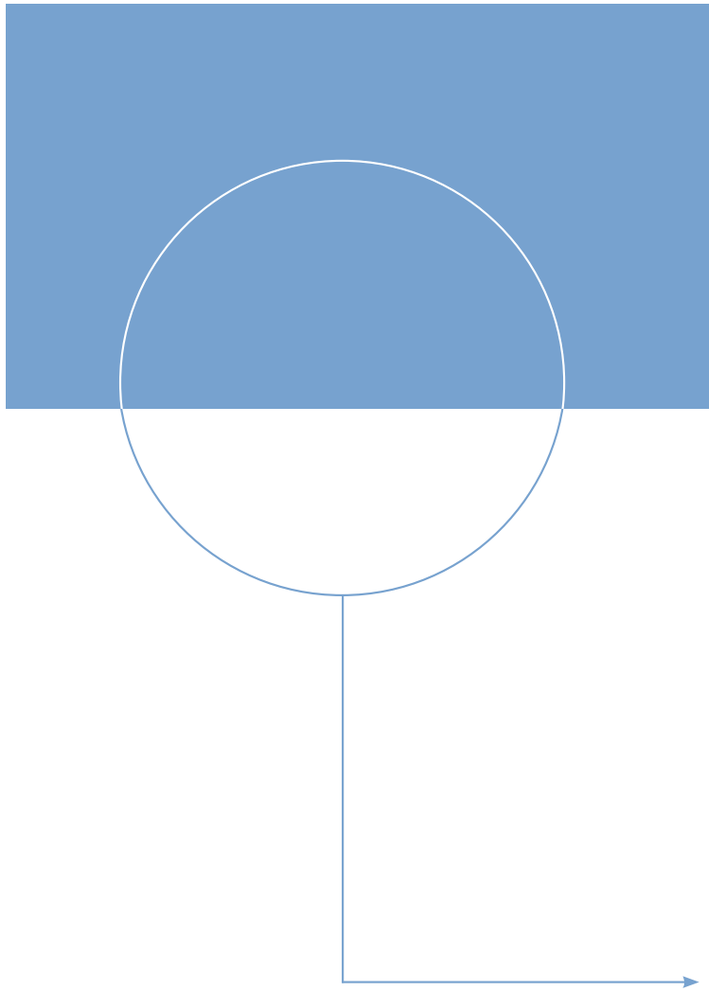

Master's thesis

2022

William Eik Hagen

NTNU
Norwegian University of
Science and Technology
Faculty of Engineering
Department of Mechanical and Industrial Engineering

William Eik Hagen

Long Term Properties of Glass Fiber Epoxy Laminates in Dry and Humid Environment

A comparison of the stress rupture failure time between saturated and non-saturated glass fiber epoxy bars

June 2022

NTNU
Norwegian University of
Science and Technology

NTNU
Norwegian University of
Science and Technology

NTNU

Norwegian University of
Science and Technology

Long Term Properties of Glass Fiber Epoxy Laminates in Dry and Humid Environment

A comparison of the stress rupture failure time between saturated and non-saturated glass fiber epoxy bars

William Eik Hagen

Mechanical Engineering
Submission date: June 2022
Supervisor: Andreas Echtermeyer

Norwegian University of Science and Technology
Department of Mechanical and Industrial Engineering

Abstract

A study of the stress rupture time of glass fiber epoxy composite laminates in humid environments was investigated. Test specimens were made in order to compare the failure time of a saturated and non-saturated specimen in distilled water for a given constant force applied. Half of the samples made were placed in a 60 °C water bath and the weight gain was recorded to find when a fully saturated state was reached. Tensile testes were performed in order to validate the mechanical properties between specimens. Then a force was determined for each test below the ultimate tensile stress and held until failure. The time to failure for each test were then plotted on a graph. Two curve fit models on the form $\sigma_c = kt^m$ was produced from the scatter points. The curve for the saturated and non-saturated specimens were then compared to estimate the difference in behavior. The saturation process converged after 2700 hours at 60 °C. The tensile performance of the saturated specimens was reduced by 66% compared to the non-saturated specimens. The amount of data on the stress rupture plots were limited given by the time available. Therefore, a lot of uncertainties can be raised to the validity and repeatability of the findings. The two curves found from the stress rupture tests showed a correlation of the tensile performance between the saturated and non-saturated specimens. From the curve fitting it was seen that the tensile performance was 63% lower for the saturated specimens. However, the slop for the saturated specimens was steeper by 57%. Based on the the number of tests performed and the variance between each test, more tests are needed to support that a change of the slope is seen for similar tests.

Contents

List of Figures

List of Tables

Symbols and Abbreviations

Table 1: Symbols

Symbol	Description	Unit
FRP	Fiber Reinforced Plastic	-
GFRP	Glass Fiber Reinforced Plastic	-
VARTM	Vacuum Infused Resin Transfer Moulding	-
UTS	Ultimate Tensile Stress	MPa
T_g	Glass Transition Temperature	K
σ_c	Constant Stress	MPa
t_f	Time to Failure	h
t_0	Pre Exponential Constant	-
ΔG	Activation Energy	$\frac{J}{mol}$
υ	Activation Volume	
R	Molar Gas Constant	$\frac{J}{Kmol}$
T	Absolute Temperature	K
K_{Ic}	Stress Intensity factor	MPa $\sqrt{m}$
A_V	Constant	-
$\dot{a}$	Crack Growth	-
n	Constant	-
Q	Crack Growth Constant	-
K_{Icf}	Start of Rapid Crack Growth	MPa $\sqrt{m}$
$M\%$	Mass Gain	-
M_t	Mass at time t	g
M_d	Mass of Dry specimen	g
C	Concentration	-
$t_{Rupture}$	Total time of Stress Rupture	h
t_{Total}	Total time of During Testing	h
$t_{Initial}$	Time for Machine to Get to Desired Value	h

1 Introduction

This master's thesis was written in the spring of 2022. When I started on my two year master's program I was introduced to test methods and mechanical understanding of composites in the course Products and Materials Testing. This inspired me to further extend my knowledge of this unexplored topic for me.

I would like to extend my gratitude towards PhD candidate Victor Maneval who helped me in the beginning with making a laminate but also throughout my thesis. Thank you to everyone in the composite group with weekly meetings and discussions of our progress. Cristian Torres, Børge Holen, Ying Qian and Marit Elinda Olaisen Odden has also helped me make testing and performing experiments in the labs much easier. Lastly I would like to thank my supervisor Professor Andreas Echtermeyer for support and help during both my specialization project as well as this master's thesis.

This master's thesis is build on the specialization project written by me, submitted December 2021 with the title *Stress Rupture Test of Glass Fiber Composites in Regards to the Long Term Properties*. Therefore, some sections uses parts of this project. Mainly the theory and setup. This was done because they share the exact same theoretical background and the master's thesis is an extension of the specialization report (Hagen 2021).

1.1 Background

Fiber reinforced plastics, FRP, have over the years become widely adopted in numerous industries. Currently maritime, offshore, aerospace, aircraft and more are using FRP composites. This is due to certain advantages and behaviors FRP composites have over more traditional structural materials such as steel and aluminium. The ability to tailor the FRP to a specific need, can be highly advantageous when it comes to product design. Moreover, FRP composites usually have an improved resistance to corrosive environments and fatigue failures over traditional materials (Nkurunziza et al. 2005).

Although FRP have some advantages over common structural materials, there are still challenges when it comes to understanding the long term durability. FRP used in marine, offshore and deep water applications are highly acceptable to humid environments. Therefore, the study of environmental aging of FRP composites is of importance, but costly and time consuming (A. E. Krauklis, A. I. Gagani, and Echtermeyer 2019). The long term properties are highly affected by the load and environmental condition they are sustaining (A. Gagani et al. 2018). Because of the viscoelastic nature of FRP, time dependant properties could produce unwanted deformation characteristics and decrease stiffness over a period of time. The behavior can be further exaggerated with different layups, humidity, temperature and loading

(Tuttle and Brinson 1986). Stress rupture testing is one method of gathering information of the long term behavior. Fitted parameters can then be used to determine the effect different factor have for the lifetime of a specimen.

1.2 Objective and Scope of the Report

The objective of this report is to get an understanding of the behavior of glass fiber reinforced plastics, GFRP, specimens saturated with distilled water compared to non-saturated specimens in regards to the stress rupture time. This is done in order to predict the long term behavior of GFRP used in maritime settings. As of writing this report, there is still little knowledge of how to estimate and predict the failure time for GFRP in terms of the stress rupture time. A general overview of the theory will be presented as well as the setup used to perform the tests. Moreover, the results and discussion will follow with future work, encountered problems and conclusion will be presented. The list below shows the overview of the contents of the thesis.

1. Overview of current Theory
2. Setup and Saturation Process
3. Results from testing
4. Discussion, encountered problems and future work
5. Conclusion

2 Theory

2.1 Stress Rupture

Stress rupture is a failure mechanism, which occurs after a certain amount of time under a constant load. To characterize stress rupture performance, a specimen is held at a constant engineering stress. Usually below the ultimate tensile stress. By performing multiple tests with varying loads, a stress-time plot can be made for the given specimen. The plot can often be regarded as linear when using a logarithmic time scale (Kinloch 2013). Stress rupture behavior is also dependant upon the temperature which the test is performed at, and by other environmental factors such as humidity (LaRochelle and Morscher 2006). The stress rupture data is useful for understanding the long term properties and could therefore aid in the design of components (Chiao et al. 1972).

2.1.1 Molecular Mechanics

Prediction of stress rupture time for polymers usually uses theory for molecular or fracture mechanics. Molecular theory focuses on the crack initiation to predict the total time to failure. This is seen as an Arrhenius equation in equation (1). ΔG and υ represents the activation energy and activation volume, respectfully. These can be seen as fitting variable and describes the temperature dependency of the fracture. σ_c is the constant stress applied and t_0 the pre exponential constant. Moreover, the molar gas constant R and the absolute temperature T is needed (Kinloch 2013).

$$t_f = t_0 \exp \frac{\Delta G - \upsilon \sigma_c}{RT} \tag{1}$$

2.1.2 Fracture Mechanics

On the other hand, fracture mechanics uses the assumption of a preexisting flaw in the material. Meaning crack initiation has already occurred. The focus is then on crack growth propagation. The stress intensity factor K_{Ic} in relation to the change in crack growth $\dot{a}$ can be seen in (2), where A_V and n are constants (Kinloch 2013).

$$K_{Ic} = A_V \dot{a}^n \tag{2}$$

To get a relationship between time and stress applied, equation (3) is used. K_{Ic} is the applied stress intensity factor and K_{Icf} is the value of the onset of rapid propagation. Q is a crack growth constant.

$$t_f = \frac{2A_v^{1/n}}{Q^2\sigma_c^2(1-2N)} \frac{n}{(1-2n)} \left[K_{Ic}^{(2n-1)/n} - K_{Icf}^{(2n-1)/n} \right] \tag{3}$$

The rupture process however, are often difficult to describe using a mathematical equation. This is because the rupture usually occurs in the non linear region of stress-strain. Therefore, test specimens are often simple such that a uniform loading of tensile stresses can be applied. The failures are predominantly caused by non local structural effects rather than the molecular or crystal structure (Chiao et al. 1972). Therefore, this study will focus on a simple power law equation to estimate the behavior. Equation (4) is therefore used where k is the intersection at $t = 1$ and m as the slope. σ_c is the constant mean stress applied in MPa while t is the rupture time in hours. k and m are fitted values and are dependant on factors such as temperature and other environmental factors (Eftekhari and Fatemi 2016).

$$\sigma_c = kt^m \tag{4}$$

2.2 Long Term Properties

Long term properties of a composites involves many different factors. (A. Krauklis 2019). The mechanical loading and the environmental factors such as temperature and humidity effects the properties of FRP composites. A typical lifetime of FRP composites are designed for 25 years of service (A. Krauklis 2019; A. E. Krauklis, Akulichev, et al. 2019). Therefore, understanding the behavior and effects during the whole life cycle could result in a better product design. Typically the long term properties for specimens in humid environments is found by comparing dry samples to samples that have been submerged and fully saturated. This will result in two different behaviors that can be interpreted in order to predict

the lifetime of specimens under similar environmental effects (A. Gagani et al. 2018). The behavior of accelerated aged specimens shows significant changes in properties compared to dry specimens. A study found the dynamic fatigue lifetime to be reduced by over a decade due to aging in hot water. The hot water made damage to the interphase between fiber and matrix, which resulted in matrix cracks propagating much faster. The failure strain was also shown to decrease with aging in water (Liao, Schultheisz, and Hunston 1999). Moreover, the tensile strength of glass fiber epoxy bars submerged in alkaline solution had a reduction of 9% after 3000h of submersion (Ali et al. 2018).

2.3 Fluid Diffusion

The diffusion rate of FRP composites has been shown to change with temperature. A higher temperature is therefore recognized to decrease the diffusion time (Fan et al. 2019). Fluid diffusion of composite laminates has proven to decrease the mechanical properties dominated by the matrix. Therefore, the FRP is expected to have reduced strength for shear and transverse loading for saturated laminates. However, the axial tensile properties has shown to not differ much from unsaturated specimens (A. Gagani 2019). For dry specimens the fibers are strongly bonded with the matrix, but the adhesion between fibers and matrix is reduced when aged in hot water. This results in poor bonding of matrix and fibers and is a leading cause of decrease in mechanical properties. This is further accelerated if the environment is corrosive to the fibers itself (Liao, Schultheisz, and Hunston 1999). A reduction of the glass transition temperature T_g is also seen for the matrix (Maxwell et al. 2005).

The diffusion rate has also shown to be faster in the fiber direction than for the transverse direction. This means the fiber orientation plays a role of the total saturation time. Firstly the free volume in the matrix are saturated before the whole laminate begins to swell due to water absorption. This could lead to swelling strains in the specimen. Composites saturated under high hydrostatic pressure showed small effect if void content was low. However, samples with higher void content was more sensitive to the pressure (A. Gagani 2019; Jiang, Kolstein, and Bijlaard 2013). The typical plot for fluid diffusion has shown to be rapidly growing at the beginning. The rate would then decrease over time until a steady state has been reached (Benmokrane et al. 2002). A Fickian model is then typically used to describe this behavior. The weight changes and time are recorded and plotted. An overestimation for the diffusion is generally seen for FRP composites. This is due to the model not taking into account swelling, and that the diffusion rate process is faster than the polymer relaxation. Because of this, the Fickian model cannot predict the volumetric changes or the stress dependant diffusion (Fan et al. 2019).

3 Materials and Setup

3.1 Materials

The glass fiber composite laminates were produced using Vacuum Assisted Resin Transfer Moulding (VARTM) as seen in figure 1. Mats of glass fiber were cut by hand and later placed on a prepared mould. A vacuum bag was placed on top with intakes on either side. One side was fitted to a vacuum machine, while the other end was placed in a bucket filled with epoxy. The epoxy would be drawn through the glass fiber mat creating a bond between fiber and epoxy. The laminate would cure for 48 hours in room temperature before moving to an 80 °C oven for 16–20 hours. The matrix epoxy was manufactured by mixing RIMR135™ resin with RIMH137™ hardener with a ratio of 100:30 by weight. Both matrix component was produced by Hexion. Specimens were then cut using a water jet. All specimens were cut to a dimension of 250 by 25 mm with a thickness of approximately 3.7 mm. All the samples tested came from the same plate. This was done in order to assume similar properties between specimens. The layup tested was [0,90,90,0].

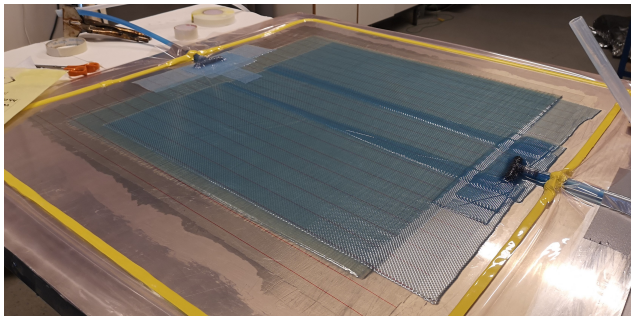

Figure 1: VARTM Process

3.2 Water Bath

Half of the specimens made were chosen to be saturated in distilled water. This was done in order to test the environmental impact water saturation has for GFRP specimens. The water bath consisted of a Cole-Parmer Polystat circulating water bath as seen in figure 2. The outlet and inlet tubes were connected to each other to form a closed loop for the water. The connected tubes were then placed in another vessel which is filled with distilled water and the specimens. The vessel is sealed with a plastic cork to prevent excessive evaporation loss. The water bath was programmed to produce 60 °C water in order to speed up the saturation process. Three samples were used as a control of the water absorption. They were weighed on a Mettler Toledo AG204 DeltaRange with a sensitivity of ±0.1 mg. The weight gain of the samples was plotted in order to spot when a fully saturated state had been achieved. The saturation was deemed complete when the change in weight had converged for all samples. An expected result from a similar study showed a fully saturated state after 1600 hours in 60 °C water with a weight gain of 0.72% (A. I. Gagani et al. 2019).

In order to secure that all the specimens were fully submerged, a regularly filling with distilled water was done. The heating process had no other functions than to speed up the saturation process. The control samples were carried in a cup filled with distilled water to the scale in order of preventing excessive loss of water. They were hand dried using paper towel until completely dry on the surface. Between each reading, the scale would be zeroed if needed. The average of the measured values were used.

The weight gain in percent was defined as seen in equation (5), where M_t is the measured value at time t and M_d is the weight of the original non-saturated sample.

$$M\% = \frac{M_t - M_d}{M_d} \cdot 100\% \tag{5}$$

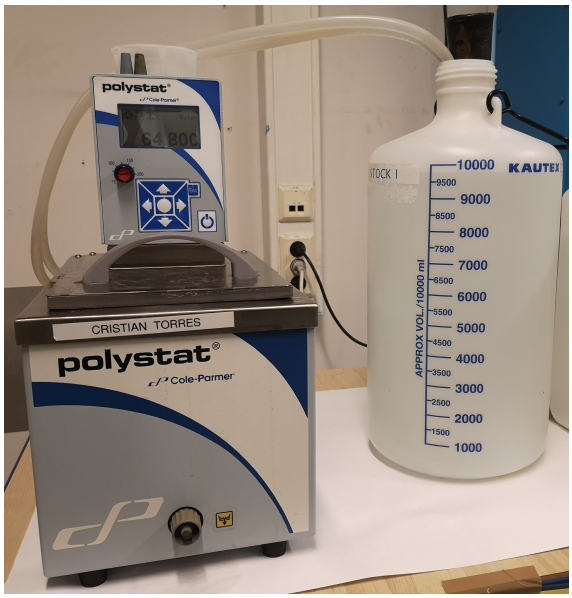

Figure 2: Water Bath on the Left with Vessel Filled with Distilled Water and Specimens on the Right

3.3 Tensile Testing

In order to obtain the ultimate tensile stress, UTS, of the specimens, an Instron 250 kN fatigue machine was used and seen in figure 3. Five samples were used to get an average peak load for the GFRP. Time, force and displacement was recorded from the machine. At a later stage when the samples chosen to be submerged in distilled water had reached saturation, the UTS was found on an MTS Landmark 50 kN machine.

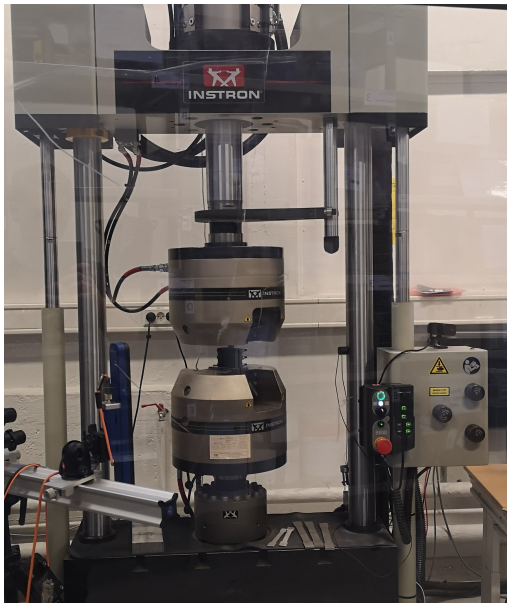

Figure 3: The Instron Machine Used During Tensile Testing for Non-Saturated Specimens

3.4 Stress Rupture Testing

To find the stress rupture failure time a MTS Landmark 50 kN machine was programmed to steadily increase the force until 90% of the desired loading. Then the force rate was reduced in order for the machine to not overshoot the target value. When the machine had reached the total force, it would maintain a constant load until total failure of the specimen. The rate of the load was determined in order to achieve 1- to 2 mm min^{-1} load rate. The time used to apply the load was subtracted from the overall time. This was done to only inspect the failure time during a constant load. Equation (6) was therefore used for all the stress rupture data. $t_{Rupture}$ indicates the time during constant load where t_{Total} is the total time and $t_{Initial}$ is the time used to apply the load.

$$t_{Rupture} = t_{Total} - t_{Initial} \tag{6}$$

During testing of the saturated specimens, a water contraption was added on the surface. A plastic sleeve was held on the surface with sticky tape. The cavity created was filled with distilled water in order to keep the specimen saturated whilst the specimen was in the machine. The loss due to evaporation would then be minimized. The contraption only covered the middle part of the specimen where failure was expected. It can be seen in figure 4.

A common issue encountered was early failures near the grips. Therefore a mesh grid and aluminum tabs were added in order to distribute the load more easily and to avoid stress concentration that would lead to early failure. This was proven to be a more effective solution to use for the non-saturated samples compared to no grip protection. However, for the saturated samples, a mesh grid provided the best results. The aluminum tabs used can be seen in figure 5 with the mesh grid in between. Duck tape was used to secure and keep the alignment when handling the specimen.

Figure 6 shows a specimen during stress rupture testing. The aluminum tabs are extended far out of the grips. Moreover, due to the clamping pressure they have begun to buckle outwards.

Figure 4: Sealed Plastic Bag Used to Hold Water During Testing

(a) Front View of Aluminum tabs with mesh

(b) Side view of Aluminum Tabs with mesh

Figure 5: Aluminum Tabs used During Stress rupture Testing

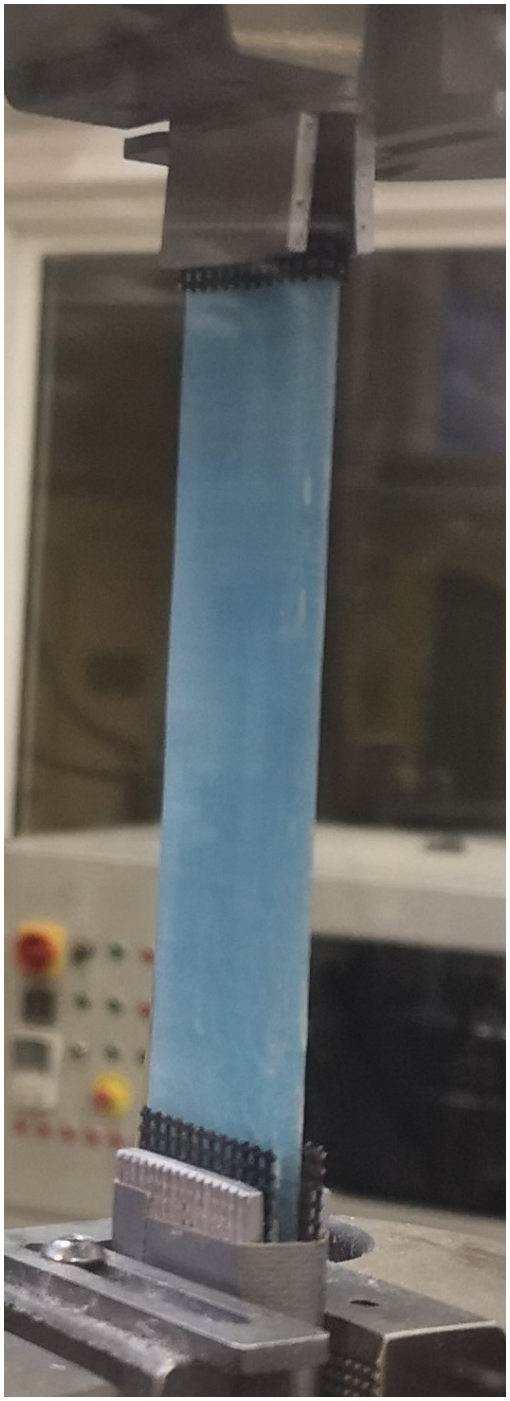

Figure 6: Specimen in Machine During Stress Rupture Test

4 Results

4.1 Water Diffusion

The percentage gain for the three reference samples saturated in distilled water were measures according to section 3. The plot of the time-weight gain can be seen in figure 7. The graph is according to the expected curve. The onset of the water intake showed a rapid intake of weight for all of the test samples with a declining curve until saturated. The maximum weight gain percentage was 0.92% while the lowest recorded was 0.69%. Three spikes after 2000 hours is seen. All of them are caused by the machine turning of. This caused the samples to gain weight. The sharp declines are when the water bath is again turned on and the saturation limit is restored. At 2700 hours all of the specimens are seen to be fully saturated at 60 °C water. The water bath machine broke after 3900 hours and the samples were left in room temperature water. At 4200 hours all of the samples had reached a new saturated value for room temperature water. The total weight gain is according to similar tests. However, the saturation time was longer than expected (A. I. Gagani et al. 2019). Visually, all of the saturated specimens had become a more transparent green color as opposed to the darker blue color of the non-saturated specimens.

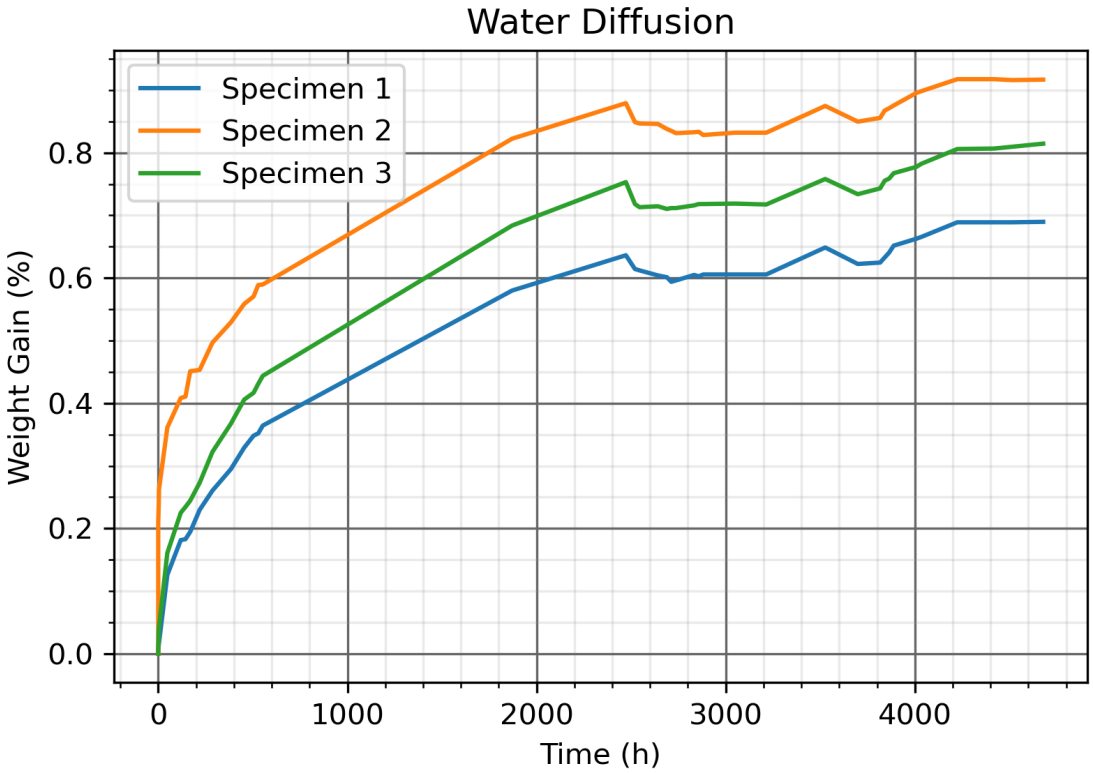

Figure 7: Water absorption

4.2 Tensile Testing

4.2.1 Non-Saturated Specimens

The theoretical strength for non-saturated specimens was calculated before testing. This was done in order to verify the results from the tensile testing but to also know the expected applied force the machine had to be capable of before testing. The theoretical values calculated can therefore be seen in table 2.

Table 2: Theoretical Strength and Force

Theoretical Tensile Strength	[0,90,90,0]
Maximum Stress (MPa)	400
Maximum Force (kN)	37.1

A total of five specimens were tested. The results of the tensile testing can be seen in figure 8. Each of the specimens had a relatively linear plot in the beginning with a sudden drop in force. Specimen 3 was the only specimen without a significant drop in its curve. This was because a failure in the grips occurred. A higher force was observed but also a much faster decrease in force once it broke. For all the tests, a distinct sound of matrix cracking and fiber failure was heard right before the break. The tests showed a clear brittle behavior when breaking.

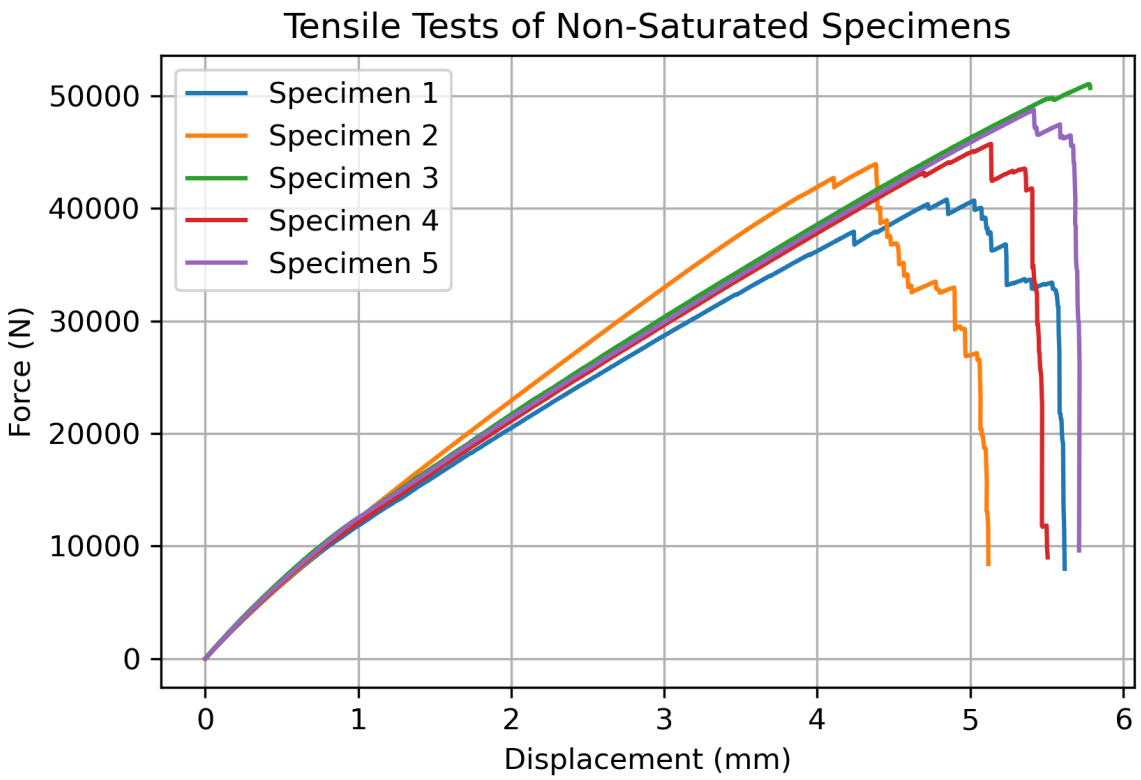

Figure 8: Force-Displacement plot for [0,90,90,0]

Table 3 displays the ultimate tensile forces gathered from the tensile tests. These values were later used to determine the forces applied during the stress rupture tests. A percentage of the mean force was then determined for each stress rupture test.

Table 3: Ultimate Tensile Force

Sample No.	Max Force(kN)
1	40.800
2	43.938
3	51.051
4	45.745
5	48.776
Mean Value	46.060

The UTS calculated for each specimen is seen in table 4. The values gathered from the machine shows an improvement of about 24% higher than the expected theoretical values.

Table 4: UTS of the Non-Saturated Specimens

Sample No.	UTS (MPa)
1	440.093
2	473.938
3	550.662
4	493.436
5	526.133
Mean Value	496.850

4.2.2 Saturated Specimens

The maximum force was also found for the saturated specimens. Originally this was not intended. However, the UTS proved to be much lower than expected from section 2.2. This meant a lot of tests were carried out intended for stress rupture ended up exceeding the UTS of the saturated samples. These tests were also used to change the rate of the load since the program was only able to control it with a force over time as described in section 3.4. The displacement-force curves for the fully saturated specimens can be seen in figure 9.

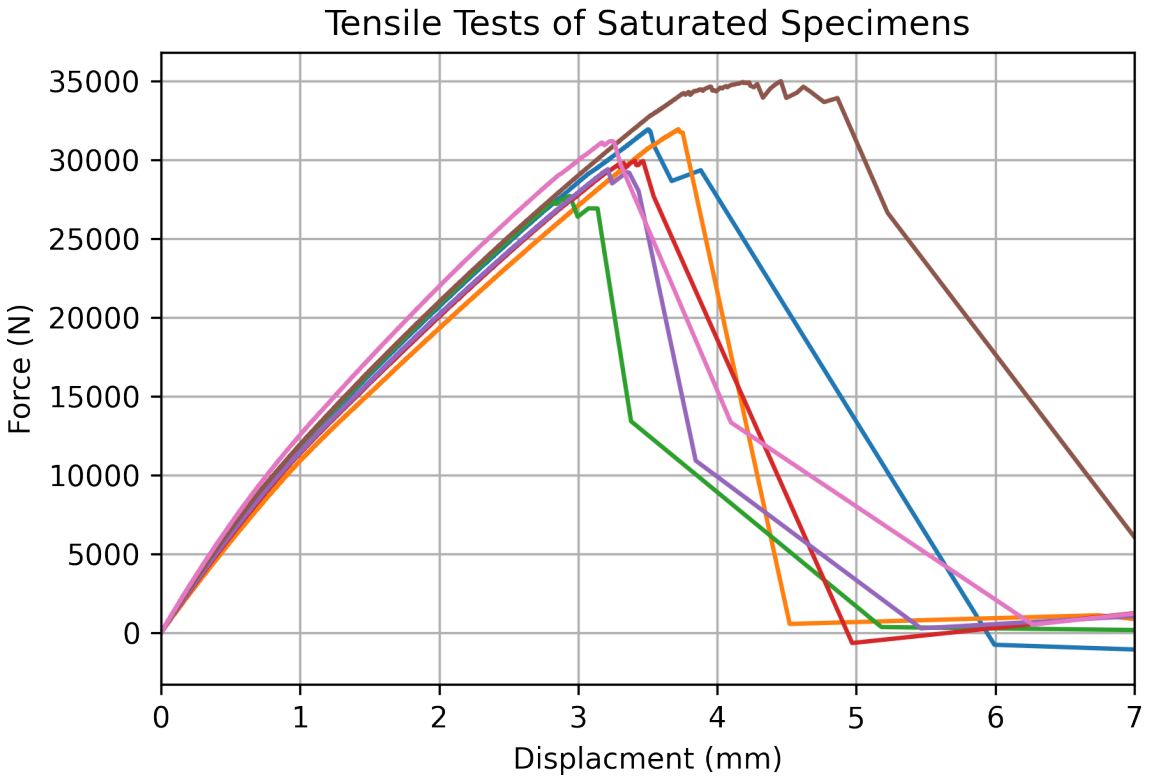

Figure 9: Tensile Test of Saturated Specimens

The UTS was then calculated based on the tensile tests. The values can be seen in table 5 as well as the mean stress. Compared to the non-saturated specimens it was found a change of 66% for the tensile performance once saturated.

Table 5: UTS for the Saturated Samples

Sample No.	UTS(MPa)
1	341.026
2	338.027
3	300.059
4	319.216
5	309.400
6	333.292
7	376.675
Mean Value	331.100

4.3 Stress Rupture

Stress rupture tests were carried out on both non-saturated and fully saturated specimens. The different stress levels were chosen based on getting a large selection of data points in regards to the available time to perform tests. Therefore, the longest test carried out took 11.5 days, while the shortest tests took five minutes before breaking. In total three valid tests were produced for the non-saturated specimens with an additional three test that slipped out of the grips. This was because the tabs slid of during testing. The groves on an aluminum tab caused by the grips can be seen in figure 11. Five failures were recorded for the fully saturated specimens. Two force-time curves are shown in figure 10 where the initial loading times vary between tests but maintains a constant force for the duration of the test. This is to illustrate the behavior of the machine. All tests showed a brittle fracture, with splintering surfaces where the fibers ruptured. This behavior can be seen in figure 16.

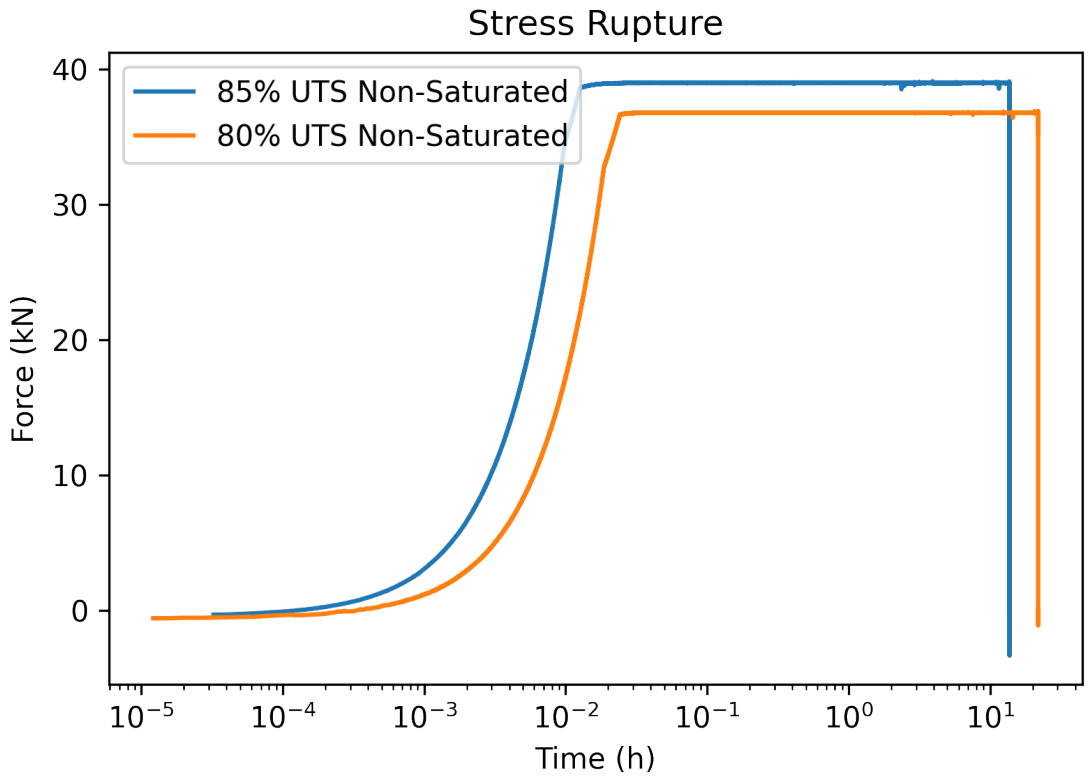

Figure 10: Stress Rupture Force over Time

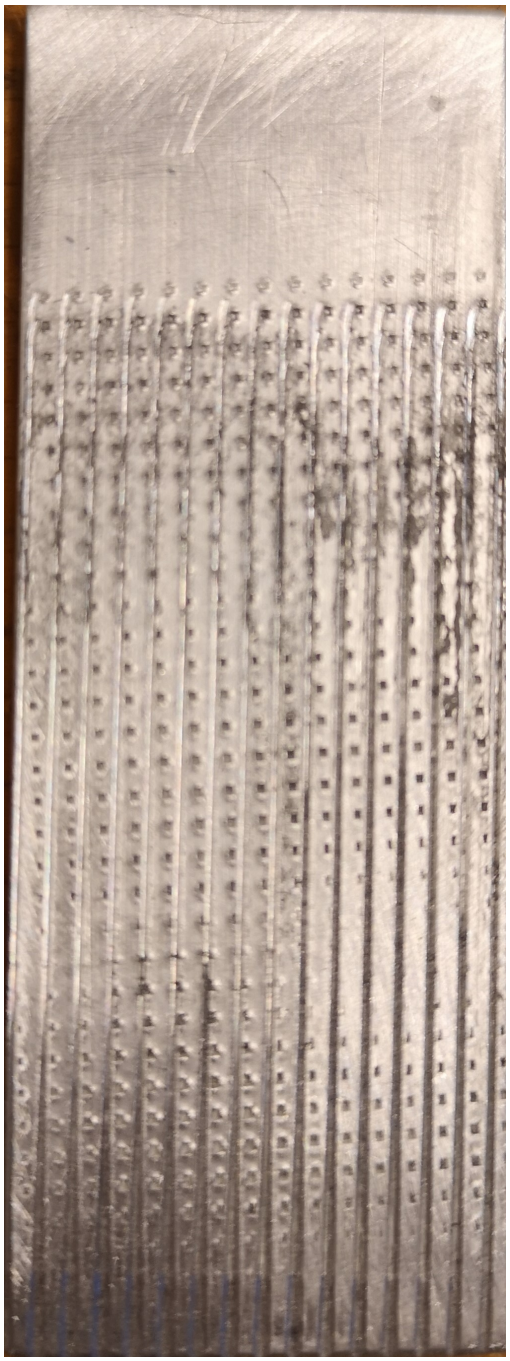

Figure 11: Marks on Aluminum Tabs after Sliding out of the Grips

A close up view of the force over time for two tests is seen in figures 12–13. Even though the machine was programmed to maintain a constant load, some variation does occur during testing. This was due to elongation and matrix- and fiber failures. Moreover, when other machines in the lab was moving, the MTS machine would be affected. The maximum deviation spotted during testing from the desired value was ±3% from the target value. Figure 14 shows the behavior of a sample that slipped out of the grips rather than breaking. A much more erratic graph is spotted compared to a graph of a securely fastened specimen.

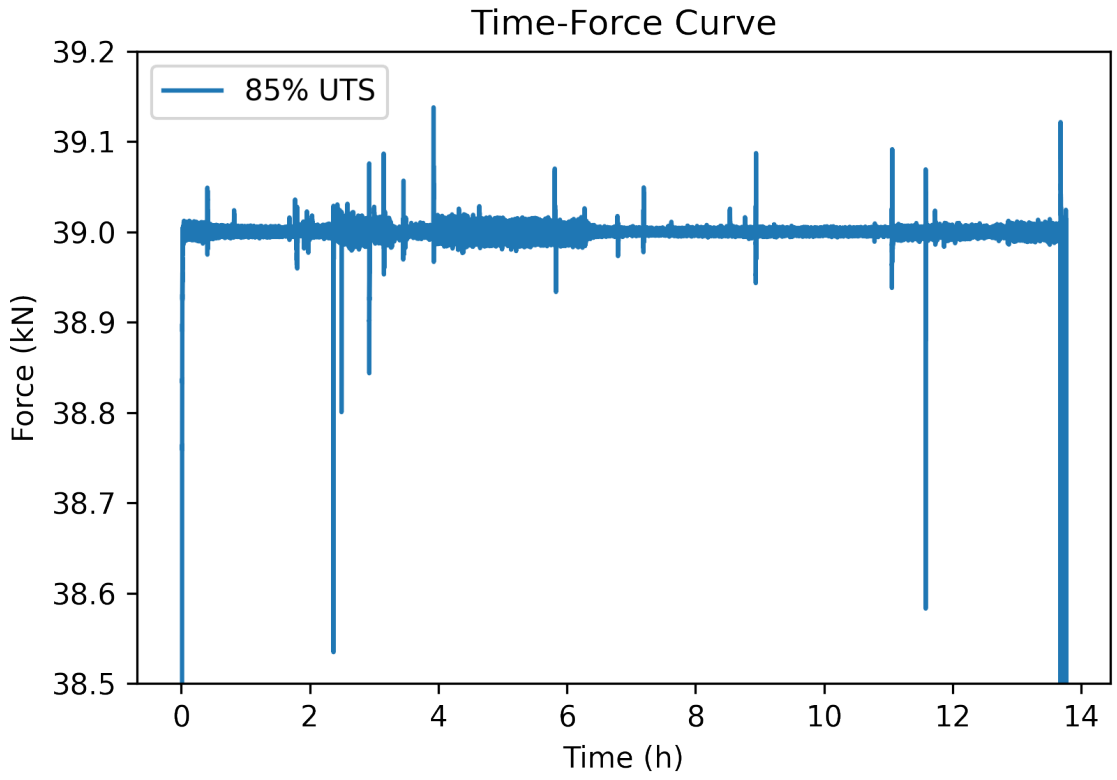

Figure 12: Close Up for test at 85% UTS for Non-Saturated Specimen

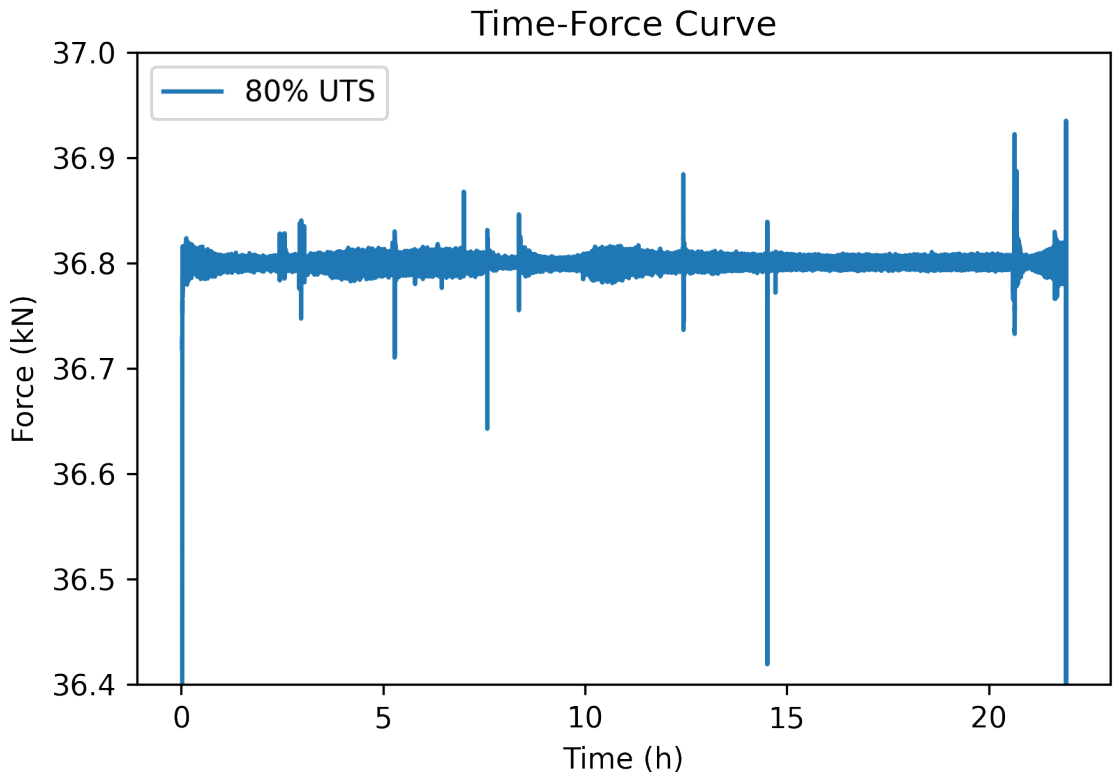

Figure 13: Close Up for test at 80% UTS for Non-Saturated Specimen

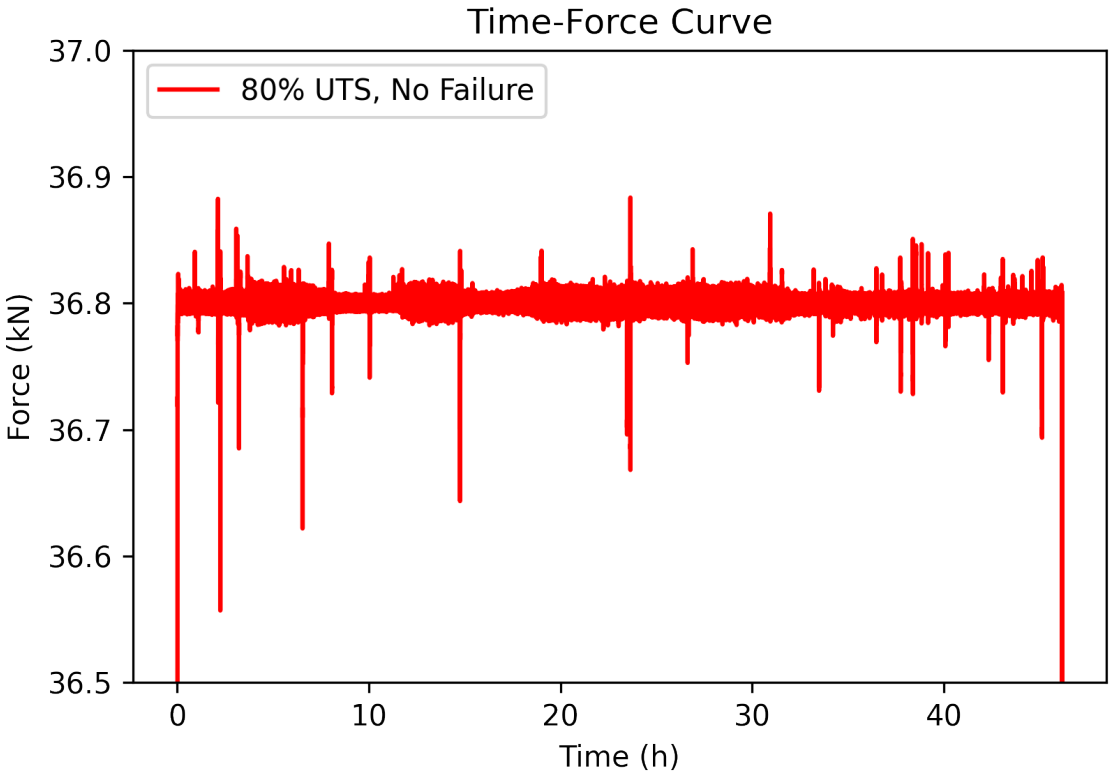

Figure 14: Close Up for test at 80% UTS with No Failure for Non-Saturated Specimen

A power law model on the form as seen in equation (7) was used to fit the experimental data gathered from the stress rupture tests. The power law equation shows a linear trend when plotted with a logarithmic time scale. Here k and m were used at fitting variables. A change in k translates the curve on the y-axis and m determines the slope of the curve. The specimens that produced no failures was not included for the behavior of the curve fitment. The constant mean stress σ_c is measured in MPa, while the time t is in hours. The curve fit is then only applicable for specimens with the same materials and under the same conditions. Visually both models share a similar trend for the slope, but the saturated models has a clear offset due to the reduced tensile performance as mentioned in section 4.2. From the formulas of the two curves in equation (7), the non-saturated curve has a change in stress after one hour of 57% taken from the k constant. Moreover, the non-saturated curve also has a steeper curve downwards of 53% compared to the non-saturated curve. At time close to zero, the curves shows a difference of 63% for the tensile strength. This is similar behavior as found for the the tensile strength of 66% in section 4.2.

$$\sigma_c = kt^m \rightarrow \begin{cases} \text{Non-Saturated Curve}: & \sigma_c = 442.5t^{-0.0355} \\ \text{Saturated Curve}: & \sigma_c = 252.7t^{-0.0543} \end{cases} \tag{7}$$

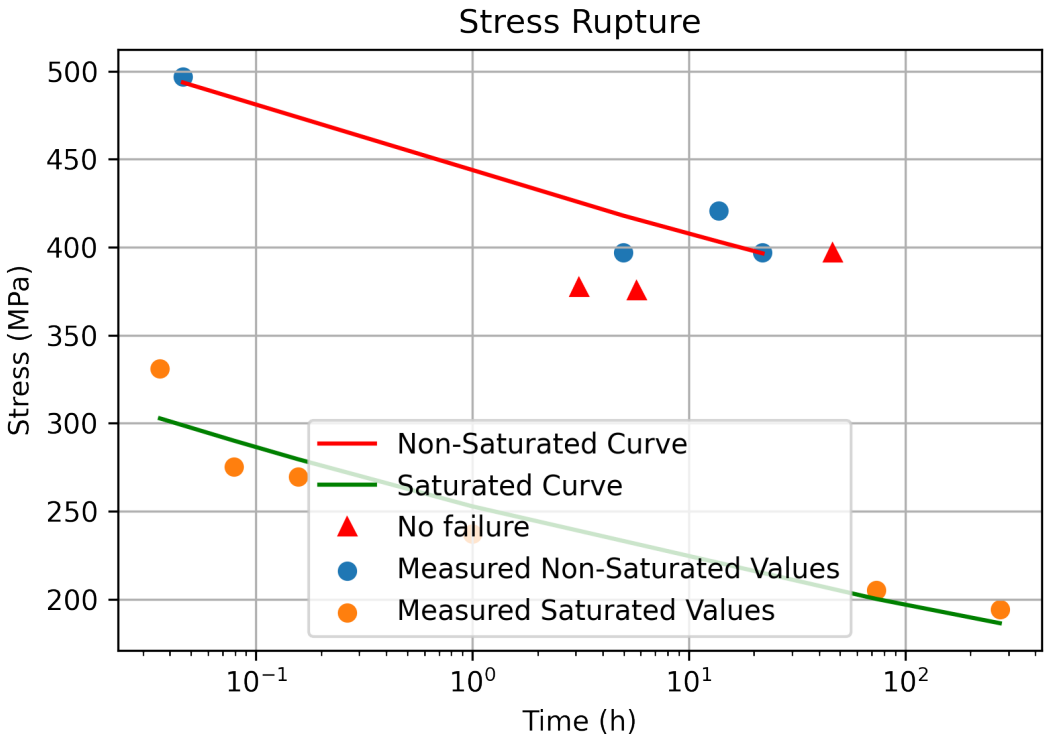

Figure 15: Stress Rupture Plot with fitted Curve

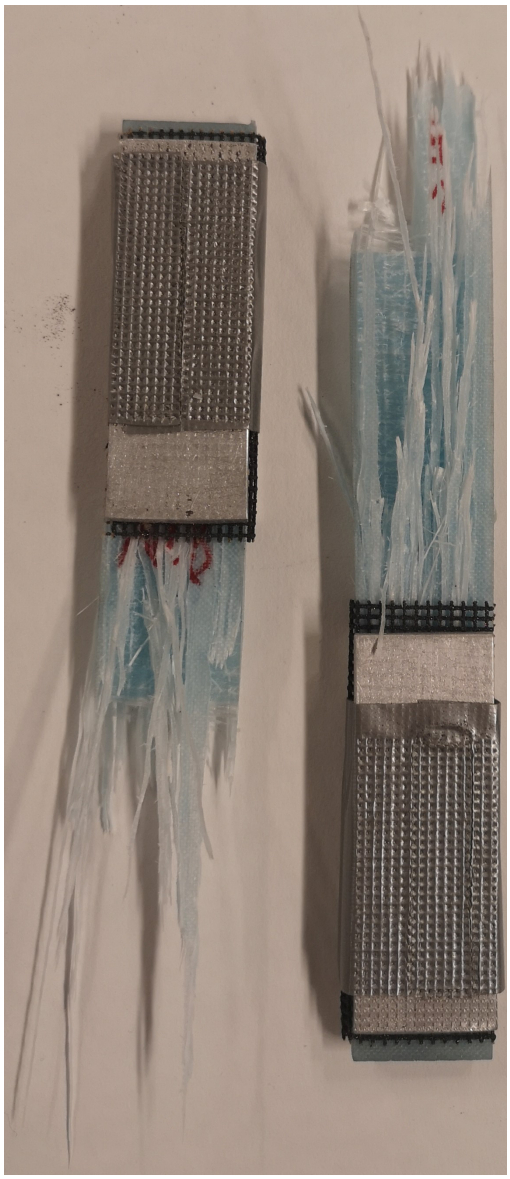

(a) Front View of Typical Rupture Behavior

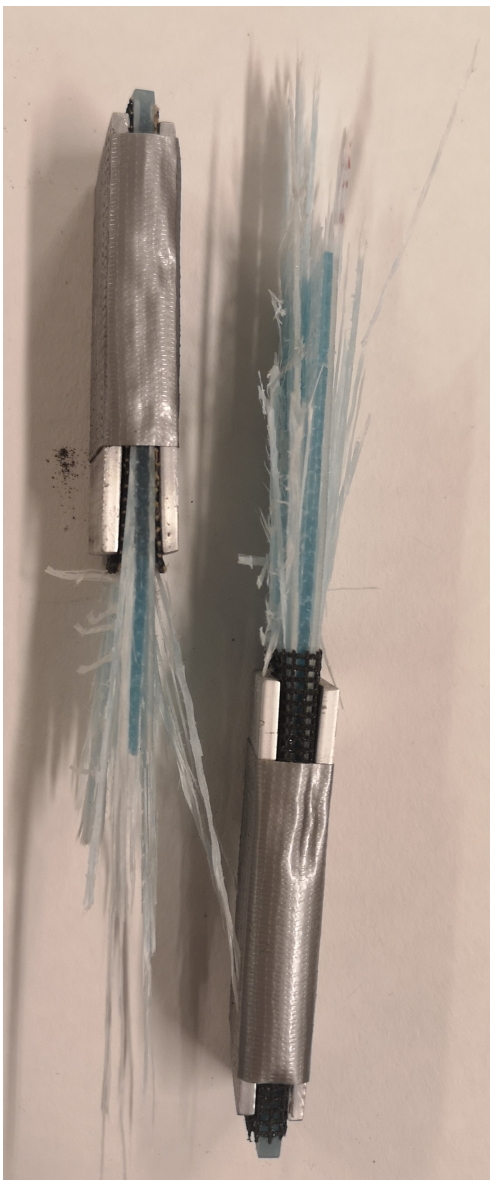

(b) Side View of Typical Rupture Behavior

Figure 16: Stress Rupture Brittle Fracture

The typical displacement curves made by the machine over the duration of the stress rupture tests can be seen in figures 17–19. All of the curves show a rapid increase of the displacement in the beginning. The displacement then progresses until a rapid increase due to breaking or slipping of the specimen. Figures 17 and 18 shows distinct plateaus where the strain is kept constant and other parts were a rapid increase is seen. However, for the specimen that did not produce failure, the graph is much smoother throughout the elapsed time as seen in figure 19.

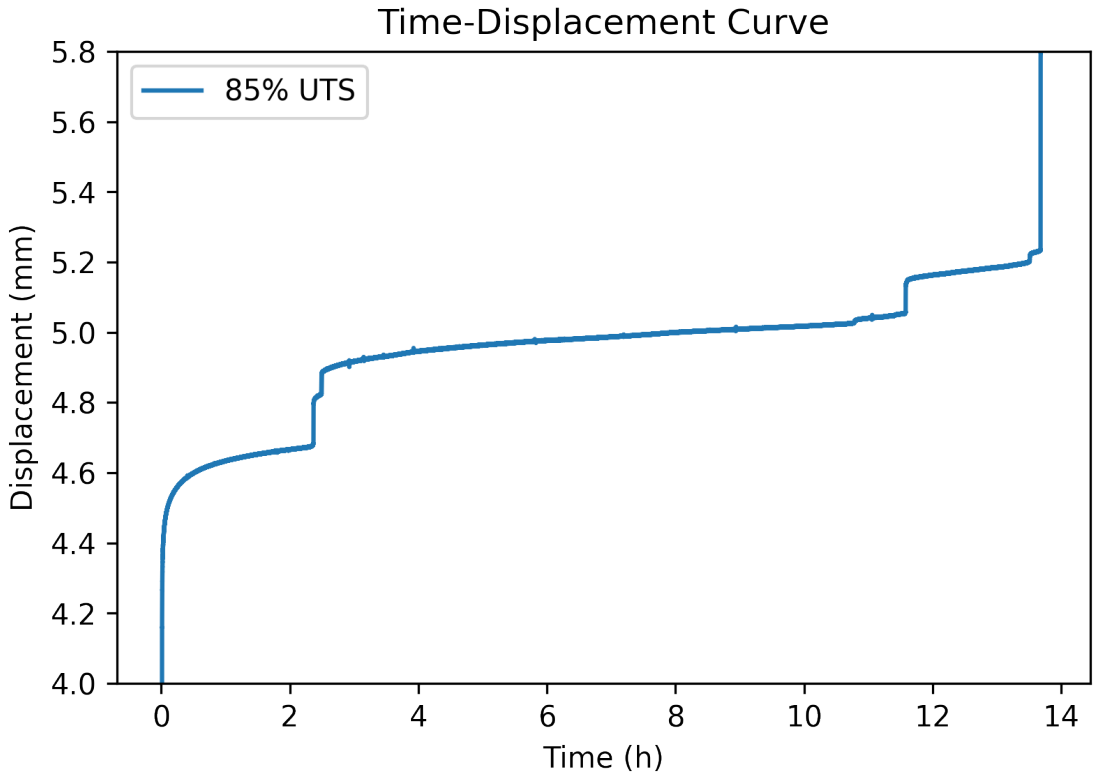

Figure 17: Machine Displacement Curve for Test at 85% UTS for Non-Saturated Specimen

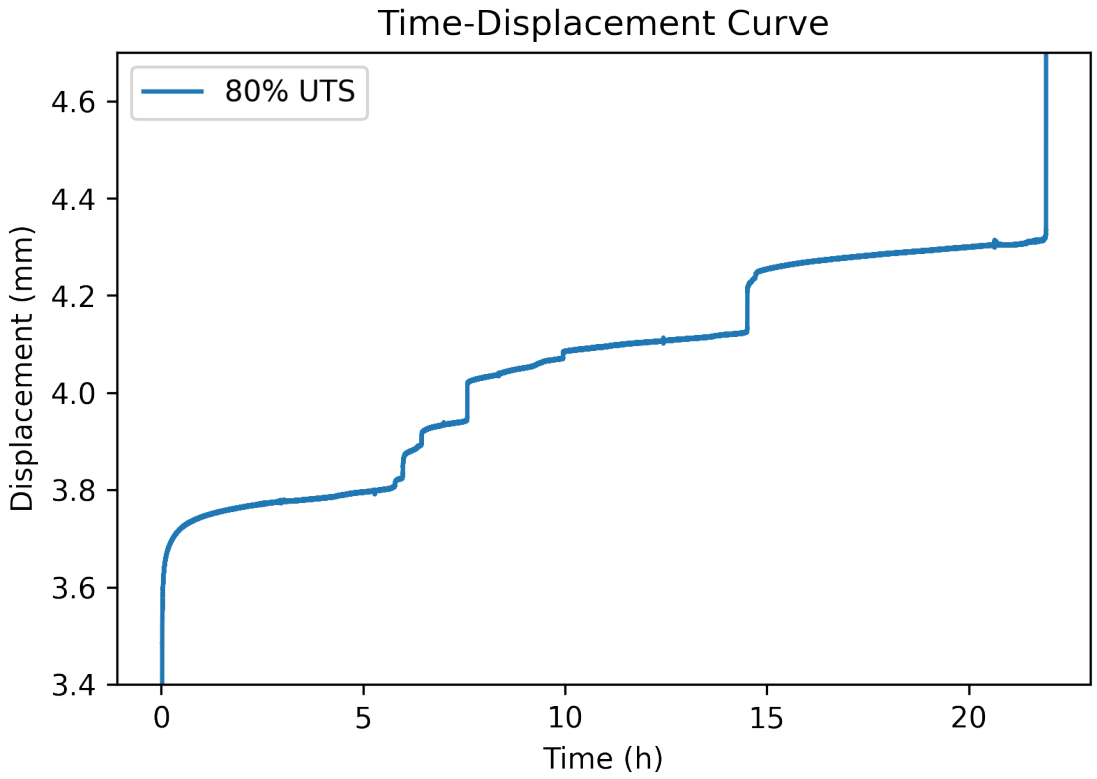

Figure 18: Machine Displacement Curve for Test at 80% UTS for Non-Saturated Specimen

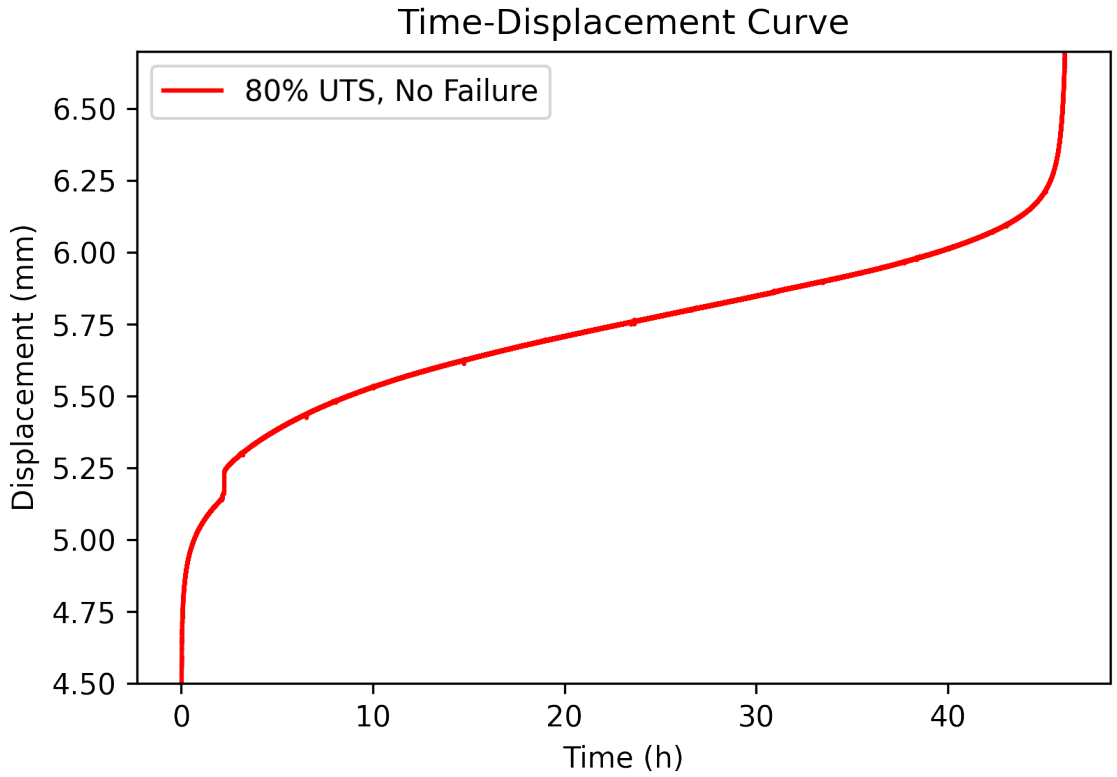

Figure 19: Machine Displacement Curve for Test at 80% UTS with No Failure for Non-Saturated Specimen

5 Discussion

5.1 Water Diffusion

The weight gain plots for the control samples showed a similar trend. However, specimen 2 had a much more rapid absorption rate in the beginning as seen in figure 7. Benmokrane et al. (2002) argued that this behavior could be explained by voids or cracks in the specimen. This would cause a sudden increase of mass, but would later follow the same curve as the other specimens. The void then allowed specimen 2 to reach the highest saturation value of 0.92% weight gain. A. I. Gagani et al. (2019) showed a similar experiment needed 1600 hours before converging. However, the converged plot showed it needed 2700 hours before fully saturated at an elevated temperature.

During the saturation process, the machine would stop running momentarily. It was then observed that the diffusion rate was slowed down. However, the total fluid concentration would go up. Two different concentration states can therefore be spotted in the graph. Right after the first saturated specimens were being used for stress rupture testing, the water bath machine stopped working. It was determined that the samples would not be affected by this since a saturated state had been achieved. Moreover, a plastic cover filled with water was used on the specimens during testing to maintain the saturated state.

In the long term, glass fibers and the epoxy will degrade due to dissolution reactions. Different elements from the specimens will therefore leach out to the water and a detectable mass loss is found. The speed of degradation is based on the surface area of the water on the specimens as well as the degradation rate constant. The degradation rate constant is affected by environmental conditions such as temperature, stress and pH (A. E. Krauklis, A. I. Gagani, and Echtermeyer 2019). This caused a more rapid degradation rate at elevated temperature which in return reduced the total mass measured. Moreover, colder water is more dense and could have increased the weight gain seen during measurements when the machine was operating at room temperature. It was also observed that the water where the specimens was placed had become oily due to the breakdown of the composites.

5.2 Tensile Testing

All of the non-saturated tensile tests showed similar behaviors. Therefore, similar properties between each specimen was estimated. Moreover, this validated the remaining specimens since they were cut from the same plate. Although the properties were matching to each other, it differed from the theoretical values calculated for section 4.2. The theoretical values used generic properties from an E-glass/epoxy. This means the theoretical values are not a perfect approximation of the test specimens. However, the theoretical properties were chosen based on similar behavior to the material used.

Similarly, the saturated samples indicated that the mechanical properties were comparable to each other. All of the samples tested showed a brittle fracture near the center of the specimen. It was used different loading rates. However, this did not impact the behavior or result. The reduction of mechanical properties was due to the degradation done to the specimens as well as increase the notch effect of the voids in the epoxy. However, other tests showed little variance in axial tensile performance where the strength is dominated by the fibers (A. Gagani 2019).

During production of the composites, there are a lot of errors that can be introduced. Contaminating of the naked fibers with fats or grease could decrease the adhesive properties to the epoxy. Air bubbles are also common fault in glass fiber epoxy specimens. The air gaps could then introduce unwanted stress concentration in form of a notch. The volume fraction of the fibers to epoxy were not measured. This could have further improved the understanding of the quality and property of the laminate.

5.3 Stress Rupture Testing

The stress rupture plot shows linear behavior as expected when plotted on a logarithmic time scale for both saturated and non-saturated specimens(Kinloch 2013). A simple power law equation as seen in equation (7) was used to predict the difference in behavior between the saturated and non-saturated samples. It was observed during testing that one of the 0 layers were not cut straight from the plate. This can be seen in figure 20 were the fibers on the right side has begun to split out due to the fibers being cut of. This was not an issue during tensile testing. This could be because the time under load is shorter compared to stress rupture testing. Therefore, this flaw was only spotted once the load had been applied after a period of time. The test machine would then detect a sudden drop in force, and would counteract to maintain a steady load.

The tensile performance showed a change in the UTS of 66% while the curve fit gave a visually estimation of a 63% change at a time close to zero hours for the non-saturated and saturated specimens. The k constant gives the stress at $t = 1$ (Eftekhari and Fatemi 2016). If a larger data set of both tensile tests and stress rupture failure times were recorded, the equations may have reflected the same difference of tensile performance. The curve for the saturated specimens have also a steeper slope. This means for a similar drop in force between the saturated and a non-saturated sample, the change in time to failure will be less for the saturated sample. The current data set is highly affected by each tests. Moreover, since the variance of failure time is large with the same force applied, the quality of the estimated curves are to be questioned. For a test of two non-saturated specimens with the same stress applied, it was noted a magnitude of 4.4 times difference in the failure time. Therefore, the lack of substantial data effects the outcome of the fitted curves. For dynamic fatigue performance it is found that the fatigue performance is not reduced or changed when saturated (Garcia-Espinel et al. 2015). However, at lower stresses the dynamic fatigue life is shortened (Shan, Lai, et al. 2002; Shan and Liao 2002). During these test for static fatigue, the lowest stress level tested was at 60% of UTS for a saturated specimen. Therefore the behavior of stress levels below this value is unknown. From the results gathered, the prediction for the long term behavior has to take into account both the drop in tensile performance but also a steeper slope for the saturated specimens. Further study needs to be conducted before this behavior can be trusted as predictable.

The displacement curves and the close up of the force over time plots are closely related to each other. For the test at 85% and 80% UTS for the non-saturated specimen, and increase in displacement is seen when a drop in power occurs. This is likely due to fiber or matrix failure, which in return lowers the force of the machine until the axial displacement has increased enough to put the specimen under the right amount of tension. However, this behavior is not seen for the test were no failure occurred. Instead figure 19 shows a smooth displacement curve while figure 14 has a more erratic behavior. The measured displacement is for the machine itself and does not display the elongation of the specimens as a strain gauge. A smooth displacement curve could then mean the specimen was continuously slipping out of

the grips, rather than an abrupt slipping due to a sudden increase or decrease in force. The close up of the force curve seen in figure 14 also backs up this theory. The more erratic behavior of the force applied indicates that the machine is constantly having to alter the force input due to the constant slipping of the specimen. This specimen was shown to have the longest lifetime. This could be because the force applied by the machine was used to drag the tabs out from the grips rather than to put tension on the specimen. One solution could be to fit specimens with a strain gauge. Then the actual strain measured is for the specimen and not the machine. This could have improved the understanding of what occurred during the test.

When performing stress rupture testing, a steady force is desired. However, the inputs from other machines was also detected during testing. This is due to the change in hydraulic power when a test is stopped or other movements of the pistons is performed by others. Therefore, the activity level in the lab was seen as a factor of how steady force the machine was able to maintain. Sudden drops and peaks of power were therefore unavoidable for the whole duration of testing. The impact for the failure time is hard to estimate and is therefore recognized as negligible. In section 4.3, this was seen as a maximum deviation of 3%. The larger drops in force seen in figures 12 and 13 might be due to failure of the matrix or fibers.

5.3.1 Tabs for Stress Rupture Testing

For stress rupture testing of non-saturated samples, aluminum tabs were necessary due to the risk of failure in the grips. The clamping force would then be more evenly distributed along the surface of the composites. A mesh grid was used in between the tabs and specimens. This was essential in order for the aluminum tabs to not slide off easily from the glass fiber epoxy specimens. The load rate was reduced and altered between some tests. This was done in order to reduce the risk of the specimens slipping. Because of the "ramp"–function used to increase the loading on the MTS machine, only a load per time was allowed to be use. Therefore, maintaining a constant displacement per time was not possible. The load per minute were chosen based on observation made during testing in order to maximum get 2 mm/min load rate. A rapid load rate was seen to produce slipping for the non-saturated samples. However, the saturated samples was not seen having issue with the loading speed. Therefore, the saturated specimens only used a mesh grid. The applied force was much lower for the saturated specimens. Failure for saturated specimens was usually concentrated towards one of the grips but the failure point was seen to usually be around 2 cm from the grip. Therefore, it is assumed that this is a natural fracture rather than the specimens being affected by the gripping pressure.

Figure 20: Split of Fibers along Right Edge

5.4 Encountered Problems

At the start of the masters thesis, it was planned to use an oven at elevated temperatures when performing stress rupture tests. This would have allowed for better understanding of the different effects surrounding environmental factors. However, even with technical support, it was not possible to get the oven working. Moreover, the saturation process took a bit longer than expected which resulted in a longer wait time before testing could occur. The MTS tensile machine also had issues where programs would not start running. This was later solved and testing of specimens were performed.

Performing stress rupture tests on the MTS machine also proved to be unreliable, especially for the non-saturated samples. Unlike the tensile tests, the stress rupture testing showed a clear favor of failure in the grip section of the machine. The solution was to change the grip pressure and to experiment with tabs and other protective methods to reduce the chance of failure or slipping of the specimens. Therefore, a lot of tests were not included as they showed a clear sign of early failures.

5.5 Future Work

For future work, the amount of valid tests need to be extended such that a clear understanding of the difference in behavior can be understood. More data would make the fitted curves more predictable for real life applications. As of now the curve is highly sensitive to the few tests performed. The inclusion of other environmental factors such as temperature and different solutions during saturation could also give a better understanding of the factors involved for the long term properties. Moreover, other factors such as UV exposure could be explored. The testing also only looked at the performance once the specimens had reached a fully saturated state. Testing throughout the saturation process could then lead to an understanding when the performance changes due to the water intake.

6 Conclusion

A fully saturated state was found after 2700 hours at elevated temperature. All of the samples used to monitor the saturation state showed similar behavior on the weight gain plot. Moreover, they were sensitive to the temperature used during saturation. A new saturated state at room temperature was reached after 4200 hours. All of the samples used for stress rupture testing was used once a fully saturated state was observed. 0.92% was the maximum weight gain and the lowest recorded was 0.69% once fully saturated.

The tensile behaviors for all of the tested specimens showed a similar trend in mechanical performance. The non-saturated specimens had a mean stress value of $\sigma = 496.85\,\text{MPa}$ while the saturated specimens had a change of 66% which gave a mean stress value of $\sigma = 331.1\,\text{MPa}$. The reduction of tensile performance was due to the saturation process, where both matrix and fibers are degraded over the time spend saturated.

The stress rupture tests showed a good prediction of the reduction of tensile stress between the saturated and non-saturated specimens at time close to zero hours. However, the slope of the saturated specimens was found to be 57% steeper. Further testing is needed to validate this behavior change. The non-saturated specimens was also found to give less reliable failures. This was due to either failure at the grips or sliding out of the grips. A lower load applied also tended to give better results with a failure at the center of the specimen.

Bibliography

Ali, Ahmed H, Brahim Benmokrane, Hamdy M Mohamed, Allan Manalo, and Adel El-Safty (2018). "Statistical analysis and theoretical predictions of the tensile-strength retention of glass fiber-reinforced polymer bars based on resin type". In: *Journal of Composite Materials* 52.21, pp. 2929–2948.

Benmokrane, Brahim, Peng Wang, Tan Minh Ton-That, Habib Rahman, and Jean-Francois Robert (2002). "Durability of glass fiber-reinforced polymer reinforcing bars in concrete environment". In: *Journal of Composites for Construction* 6.3, pp. 143–153.

Chiao, T. T., Jay K. Lepper, Norriss W. Hetherington, and R. L. Moore (1972). "Stress-Rupture of Simple S-Glass/Epoxy Composites *". In: *Journal of Composite Materials* 6, pp. 358–370.

Eftekhari, Mohammadreza and Ali Fatemi (2016). "Creep behavior and modeling of neat, talc-filled, and short glass fiber reinforced thermoplastics". In: *Composites Part B: Engineering* 97, pp. 68–83.

Fan, Yiming, Antonio Gomez, Serena Ferraro, Brian Pinto, Anastasia Muliana, and Valeria La Saponara (2019). "Diffusion of water in glass fiber reinforced polymer composites at different temperatures". In: *Journal of Composite Materials* 53.8, pp. 1097–1110.

Gagani, Abedin (2019). "Environmental Effects on Fiber Reinforced Polymer Composites Fluid and Temperature Effects on Mechanical Performance". In.

Gagani, Abedin, Yiming Fan, Anastasia H Muliana, and Andreas T Echtermeyer (2018). "Micromechanical modeling of anisotropic water diffusion in glass fiber epoxy reinforced composites". In: *Journal of Composite Materials* 52.17, pp. 2321–2335.

Gagani, Abedin I, Anna B Monsås, Andrey E Krauklis, and Andreas T Echtermeyer (2019). "The effect of temperature and water immersion on the interlaminar shear fatigue of glass fiber epoxy composites using the I-beam method". In: *Composites Science and Technology* 181, p. 107703.

Garcia-Espinel, JD, D Castro-Fresno, P Parbole Gayo, and F Ballester-Muñoz (2015). "Effects of sea water environment on glass fiber reinforced plastic materials used for marine civil engineering constructions". In: *Materials & Design (1980-2015)* 66, pp. 46–50.

Hagen, William Eik (Dec. 2021). "Stress Rupture Test of Glass Fiber Composites in Regards to the Long Term Properties". Specialization Project at NTNU.

Jiang, Xu, Henk Kolstein, and Frans SK Bijlaard (2013). "Moisture diffusion in glass–fiber-reinforced polymer composite bridge under hot/wet environment". In: *Composites Part B: Engineering* 45.1, pp. 407–416.

Kinloch, Anthony James (2013). *Fracture behaviour of polymers*. Springer Science & Business Media.

Krauklis, Andrejs (2019). "Environmental Aging of Constituent Materials in Fiber-Reinforced Polymer Composites". In.

Krauklis, Andrey E, Anton G Akulichev, Abedin I Gagani, and Andreas T Echtermeyer (2019). "Time–temperature–plasticization superposition principle: Predicting creep of a plasticized epoxy". In: *Polymers* 11.11, p. 1848.

Krauklis, Andrey E, Abedin I Gagani, and Andreas T Echtermeyer (2019). "Long-term hydrolytic degradation of the sizing-rich composite interphase". In: *Coatings* 9.4, p. 263.

LaRochelle, Kevin J and GN Morscher (2006). "Tensile stress rupture behavior of a woven ceramic matrix composite in humid environments at intermediate temperature—part I". In: *Applied Composite Materials* 13.3, pp. 147–172.

Liao, Kin, Carl R Schultheisz, and Donald L Hunston (1999). "Long-term environmental fatigue of pultruded glass-fiber-reinforced composites under flexural loading". In: *International journal of fatigue* 21.5, pp. 485–495.

Maxwell, AS, WR Broughton, GD Dean, and GD Sims (2005). "Review of accelerated ageing methods and lifetime prediction techniques for polymeric materials." In.

Nkurunziza, Gilbert, Brahim Benmokrane, Ahmed S Debaiky, and Radhouane Masmoudi (2005). "Effect of sustained load and environment on long-term tensile properties of glass fiber-reinforced polymer reinforcing bars". In: *ACI structural journal* 102.4, p. 615.

Shan, Ying, Kian-Fong Lai, Kai-Tak Wan, and Kin Liao (2002). "Static and dynamic fatigue of glass–carbon hybrid composites in fluid environment". In: *Journal of composite materials* 36.2, pp. 159–172.

Shan, Ying and Kin Liao (2002). "Environmental fatigue behavior and life prediction of unidirectional glass–carbon/epoxy hybrid composites". In: *International journal of fatigue* 24.8, pp. 847–859.

Tuttle, Mark E and Hal F Brinson (1986). "Prediction of the long-term creep compliance of general composite laminates". In: *Experimental Mechanics* 26.1, pp. 89–102.